Journal of Cell Science 106, 473-484 (1993)
Printed in Great Britain © The Company of Biologists Limited 1993

The differentiation and lineage development of goblet cells in the murine small intestinal crypt: experimental and modelling studies

Ursula Paulus[1], Markus Loeffler[1,*], Joachim Zeidler[1], Gary Owen[2] and Christopher S. Potten[2]

[1]Department of Biometry, Medizinische Universitaetsklinik, LFI-Ebene 5, Joseph-Stelzmann Strasse 9, D5000 Koeln 41, Germany
[2]CRC Department of Epithelial Biology, Paterson Institute for Cancer Research, Christie Hospital (NHS) Trust, Wilmslow Road, Manchester, M20 9BX, UK

*Author for correspondence

SUMMARY

The objective of this study was to provide a new insight into the origin and lineage development of mucus-producing cells in the small intestinal crypt. For this, new experimental data were obtained from both crypt sections and whole mounts. Model simulation studies were undertaken to investigate which rules are most likely to govern the dynamic cellular development and goblet cell pedigree.

We have measured the frequency of mucus-secreting goblet cells (using alcian blue and periodic acid Schiff's stains) at each cell position in the ileal murine crypt. These measurements, made on sections, overestimate the number of goblet cells because of the size and centripetal position of the stained cytoplasm. The correction factor for this overscoring has been measured to be 0.25 by two independent methods. The data suggest that there are about 12 functional goblet cells per crypt many of which retain an ability to divide. We have also determined the labelling index of the crypt goblet cells at each cell position. Spatially, goblet cells exhibit a small degree of clustering in the crypt and show a good mixture with columnar cells.

We have adapted our earlier dynamic matrix-based computer simulation model to take into account goblet cell differentiation. The modelling suggested the following conclusions: firstly, goblet cells do not have their own stem cells but share a common stem cell with the columnar cells; secondly, the goblet lineage differentiates from the transit population two to three generations before the end of the lineage; and thirdly, the decision to switch on goblet properties is stochastic at a specific step in the development of columnar cells.

Key words: goblet cells, differentiation, proliferation, model

INTRODUCTION

Mucus secreting, or goblet cells, were first described in the gastrointestinal system by histopathologists at the end of the last century (Bizzozero, 1892; Sacerdotti, 1894). These cells produce and secrete in an apocrine fashion mucopolysaccharides of either a neutral or acidic nature. Mucus production clearly begins in the crypt, and the mature mucus-secreting cells migrate in a coordinated fashion with the columnar epithelial cells on to the villus. In both crypt and villus they produce their differentiated product, which aids in the smooth passage of material down the intestine. The number of goblet cells varies significantly along the gastrointestinal tract (Cheng and Leblond, 1974; Merzel and Leblond, 1969; Cheng, 1974).

Cell kinetic studies associated with the goblet cell lineage in mice have indicated that differentiated goblet cells containing mucopolysaccharides retain the ability to undergo DNA synthesis and can be labelled with tritiated thymidine and be observed in autoradiographs. This work owes much to the seminal studies of Leblond and collaborators who noted that the more primitive and proliferating goblet cells can be observed in the lower regions of the murine crypt. They also proposed that the goblet cells differentiate via a discrete lineage, but have a common ancestral stem cell with the columnar epithelial cells and the Paneth cells (Leblond and Messier, 1958; Merzel and Leblond, 1969; Merzel and Almeida, 1973; Cheng, 1974; Cheng and Leblond, 1974). Similar observations have been made in the large bowel (Chang and Leblond, 1971; Chang and Nadler, 1975). The concept of a goblet cell lineage originating from a common ancestral stem cell was based initially on: (1) the observations that the proliferating oligomucous cells (the more primitive goblet cells) were primarily in the lower regions of the crypt, and (2) the appearance of labelled cytoplasmic markers (phagosomes) that were initially generated at the base of the crypt where the stem cells are located and then appeared in the various crypt cell lineages at times that were consistent with the measured turnover time of the various lineages, including

the goblet cell population (Cheng and Leblond, 1974). This has been further supported by studies of regenerated crypts following radiation injury (Inoue et al., 1988; Potten, 1990) and studies on embryo aggregation chimeras, mutation studies, and transgenic mouse studies (Gordon et al., 1992).

In spite of the passage of virtually a century since their initial description, details of their precise numbers per crypt, how these numbers change during cellular maturation and migration and where exactly the goblet cell lineage differentiates from the columnar cell lineage remains largely obscure. Cooper (1974) estimated from whole crypt squashes that there were about 17.5 mature goblet cells per ileal crypt (or 7% of the epithelial cells) that could be stained by alcian blue (AB). The mucus in goblet cells can be stained by alcian blue or by the periodic acid/Schiff's (PAS) staining technique. The mucous areas in the cytoplasm that are stained by these reagents are centripetally positioned in terms of the crypt, i.e. they are close to the lumen. The size of these stained areas depends on the position of the section in relation to the goblet cell and also, in all probability, on the degree of maturity of the goblet cell. The centripetal position and the size of these positively stained areas influence counts made on the number of goblet cells in sections cut through the intestine in a manner similar to that described for mitotic figures (Tannock, 1967; Potten et al., 1988).

We have demonstrated recently that a large body of experimental data on crypt sections can consistently be explained by a pedigree model for the columnar cell development, which also describes the temporal and spatial dynamics of the system (Loeffler et al., 1986, 1988; Potten and Loeffler, 1987). This simulation model, based on a matrix arrangement, links the lineage of cells and cell migration in such a way that the spatial arrangement of cells and the degree of vertical and lateral cell movement in the crypt can be explained in a quantitative way. The model also accommodates the stem cell concept, since these cells are placed in the model immediately above the Paneth cells. However, the simulations performed to date do not take into account goblet cell differentiation and hence, one of our objectives here was to incorporate the differentiation and lineage development of the goblet cells. This will result in a further sophistication of the model making it more realistic and also provide some insight into goblet differentiation and lineage development. In another recent model refinement we concluded that the number of actual stem cells giving rise to the epithelium should not be much larger than eight in a small intestinal crypt. This conclusion was based on the analysis of data provided by Winton et al. (1988) on the spatial spread of the progeny of stem cells with a negative staining for a lectin binding marker (Dellanna et al., 1989).

The objectives of the present study were to determine at what point in the lineage the goblet cell branch was initiated and how many transit divisions occur within its pedigree. In order to investigate this question, we have undertaken further experiments and detailed histological measurements on: (1) the number and position of the goblet cells in sections; (2) whether or not the nuclei underlying the positive staining cytoplasm are in S-phase; (3) detailed measurements of the position of the positive staining mucus region on the radial axis of the crypt; (4) the size of this mucous area; and (5) the number of goblet cells in whole crypts and the proportion of goblet cells on the villus. We have then adapted our dynamic spatial model of the crypt and undertaken simulations of the goblet cell pedigree and the spatial distribution of the goblet cells in the crypt.

MATERIALS AND METHODS

Animals

Male BDF1 mice between the ages of 10 and 12 weeks were housed under conventional conditions, with food and water ad libitum, and were used in groups of 4 animals at a time. They were kept under conditions of controlled lighting with the lights on for a period of 12 hours starting at 0700 hours. At 40 minutes before sacrifice the animals were injected intraperitoneally with 0.925 MBq of tritiated thymidine ([^{3}H]TdR).

Histological procedures

Segments of the small intestine (ileum) were removed. The contents were gently extruded and the samples were fixed in either formalin-saline or Carnoy's fixative, the former for 24 hours and the latter for 20 minutes, after which material was stored in 70% ethanol until required. Prior to histology, the pieces of intestine were further cut into segments, bundled together in surgical tape (Potten and Hendry, 1985), embedded in either resin (hydroxypropyl methacrylate) or paraffin and sectioned at 1 μm and 3 μm, respectively. The sections were stained with alcian blue (AB), combined AB plus periodic acid/Schiff's (PAS) (AB + PAS), or PAS alone. Thus, each mouse provided 12 different sections (2 fixatives, 2 types of embedding material and section thickness and 3 different stains). All sections were counterstained with haematoxylin. The AB detects acidic mucopolysaccharides and the PAS detects neutral mucopolysaccharides. In practice, virtually all goblet cells in the crypt were stained with either AB or PAS and, therefore, all appeared in the sections stained with PAS + AB as blue or purple cells. The PAS stains the Paneth cells pale pink and the formalin-saline fixation retained the granules in the Paneth cells while the Carnoy's fixative tended to dissolve or remove the granules. From the 12 sections per mouse, counts of goblet cells were performed on the PAS + AB-stained, formalin-saline-fixed, resin-embedded sections, which proved most satisfactory.

Whole mount preparations

Additional segments of the ileum were fixed in formal-saline, transferred to 70% ethanol and used for crypt and villus isolation. This was achieved by hydrolysis in 5 M hydrochloric acid for one hour at room temperature and a mechanical fragmentation of the mucosa into crypts and villus fragments. A micropipette was then used to pick up either intact crypts or intact villi, which were then stained with either a 0.1% solution of AB in 5% aluminium sulphate for a minimum of 90 minutes or combined 1% alcian blue with PAS.

Scoring procedure

From the transverse sections of the intestine, good longitudinal sections of the crypts were selected and the position of each cell along the sides of the crypt column and the position of PAS + AB positive cytoplasm were recorded using the crypt positional scoring programme as described elsewhere (Potten et al., 1982; Kaur and Potten, 1986; Potten et al., 1992; Li et al., 1992). In this way, the position and total number of goblet cells were recorded

for 50 half-crypt sections per mouse and, since there were 4 mice in total, this gave a total of 200 half-crypt sections analysed. Also recorded was the spatial relationship between goblet cells, i.e. whether they occurred singly, or as pairs, triplets, etc. The position of tritiated thymidine-labelled nuclei was also recorded on a cell positional basis at the same time. Thus, a frequency plot of

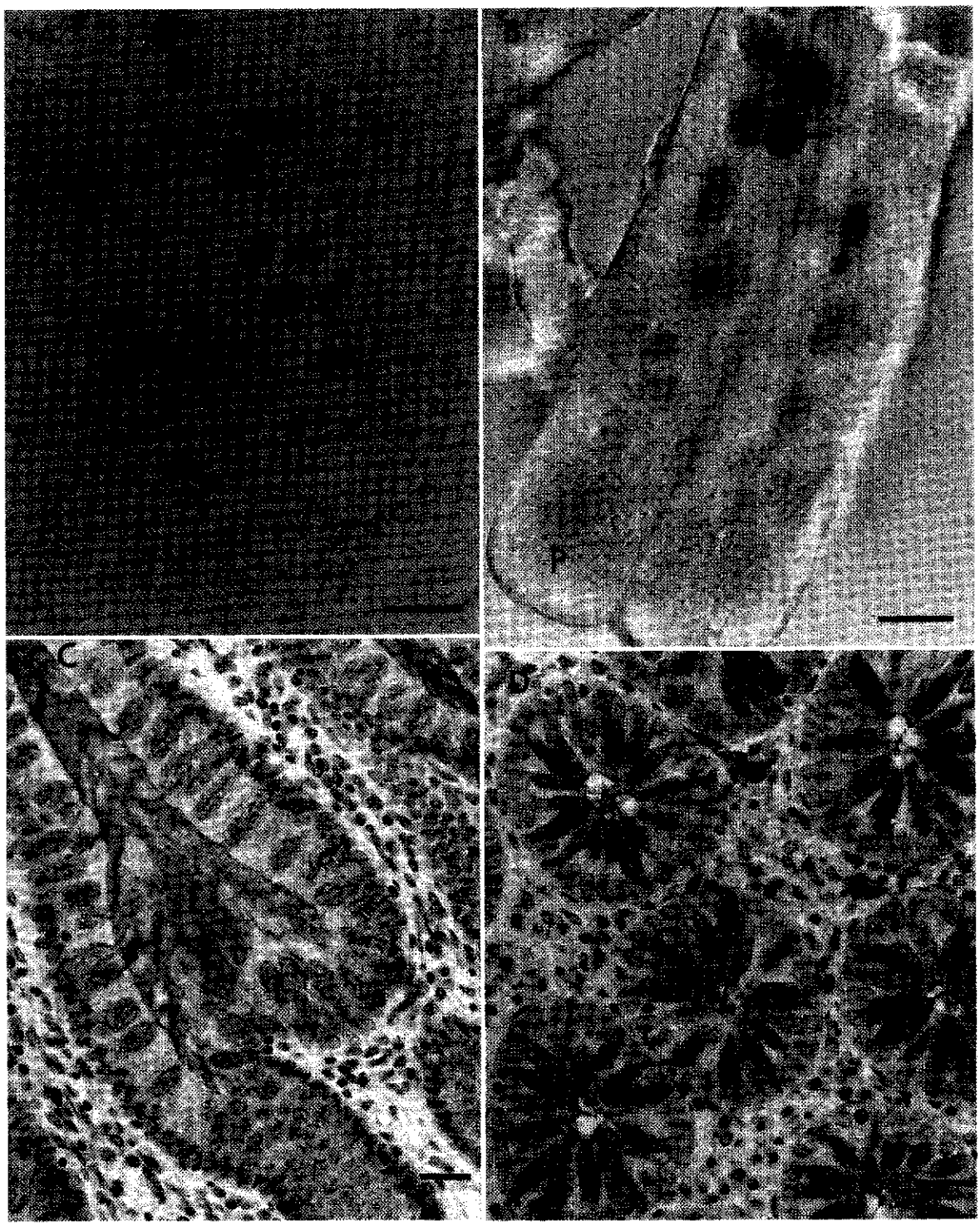

Fig. 1. Examples of experimental preparations. (A) 1 μm resin sections of mouse ileum stained with periodic acid Schiff's. The mucous cells, centripetally positioned, can be seen easily (arrows); m, mitotic figures; P, Paneth cells. (B) Isolated whole crypts stained with alcian blue to show the total number of goblet cells (arrow) accumulated when optically sectioned through the entire crypt (P, Paneth cells). (C) 3 μm paraffin sections stained with haematoxylin and alcian blue of human small intestine showing the greatly increased frequency of goblet cells (blue) and mucus secretion into the lumen of the crypt (L, lumen). (D) 3 μm paraffin section cut transversely across the crypts in the human colon showing the numerous blue-stained goblet cells present. Such additional sites can be analysed further with the model described herein (L, lumen of the crypt). Bars, 20 μm.

the total number of goblet cells or labelled goblet cells at each position could be obtained.

The whole-crypt preparations were viewed without squashing by optically sectioning through each crypt and recording the total number of blue-stained mucus-secreting cells per crypt (see Fig. 1). A total of 100 crypts were analysed in this way for the entire group (approximately 25 per mouse). The whole-villus preparations were also viewed microscopically without squashing. Areas of the surface of the villi were arbitrarily defined, and differential scores of blue-stained mucus-secreting cells and all other cells were made. Again, 100 such areas on the villi were analysed for the entire group (approximately 25 per mouse), which resulted in over 10,000 epithelial cells being scored.

Determination of the correction factor (f_T)

Two methods were used to determine the value of the factor by which goblet cells in longitudinal sections are overscored.

The first method involves a calculation of the factor based on measurements of the size and positioning of cell nuclei and mucous body. The details of this method are strictly analogous to the procedure given for correction of mitotic figure counts (see Tannock, 1967; Potten et al., 1988). Fig. 2 gives a schematic summary of the parameters that need to be obtained from longitudinal and transverse sections of crypts. Using the resin sections the size and radial position of the mucus-stained areas in each cell were measured with a calibrated eyepiece micrometer. This was performed on 25 goblet cells in total. The figure legend gives the values actually observed and the appropriate formula for f_T.

The second method used for determining f_T relates the ratio of goblet cells to all cells found in whole crypts to the ratio of goblet cells to all cells seen in crypt sections (see Potten et al., 1988). The correction factor is applied in subsequent presentations to adjust the numbers of goblet cells.

Description of the simulation model

Model assumptions

The model we used here is an extension of a previously published model (Loeffler et al., 1986, 1988; Potten and Loeffler, 1987). Briefly, we will summarise the basic assumptions and describe how we extend them to incorporate the goblet cell lineage.

Previous model assumptions

(1) Geometry. It is assumed that the crypts can be adequately described by a two-dimensional array of cells with cylindrical boundary conditions. The crypts are assumed to have a height of 24 cells and a circumference of 16 cells. Each model cell has four neighbouring cells giving a matrix representation of the crypt. The tapering of the crypt at its base is accounted for by vacant cell positions.

(2) Pedigree. The first few positions in the crypt are occupied by non-proliferating Paneth cells (P cells). The rest of the crypt cells develop from actual stem cells (A cells) that are located immediately above the Paneth cells. The number of actual stem cells is assumed to be within the range of four to eight per crypt. The stem cells are assumed to divide asymmetrically giving rise to differentiated transit (T) cells, which mature further as they migrate (T1, T2, TL cells). It is assumed that these T cells undergo a predetermined number of symmetric cell divisions (L) giving rise to 2^L non-dividing mature (M) descendants. This gives a pedigree or lineage concept for the cell differentiation process with an implicit aging of the T cells associated with a specific number of cell divisions.

(3) Cell kinetics. The Paneth cells and mature cells do not divide. The stem cells (A cells) are assumed to have a cycle time of 16 hours on average with a range of 12-20 hours and an S-phase duration of 9 hours. The transit cell population has a cycle

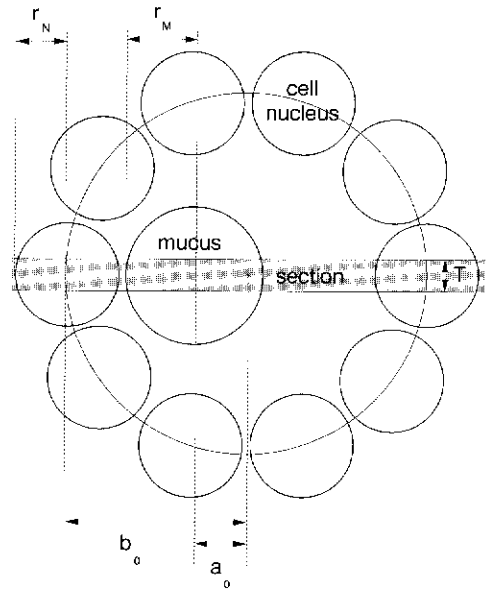

Fig. 2. Diagram showing the correction for centripetal position and the size of the mucus-staining region of a goblet cell; a modified version of the Tannock correction factor. a_0 - this is the average radial position to the centre of the mucus staining region as measured in longitudinal section but viewed here in transverse section. The measured parameter is 3.9 μm ± 0.4 (mean ± s.e.m.). b_0 - this is the average radial position of the cell nuclei at the edge of the crypt in longitudinal section, which is measured to be 13.9 μm ± 0.6. r_N - this is the average radius of a columnar cell nucleus in transverse sections, which is 3.6 μm ± 0.18. r_M - this is the average radius of the stained area of mucus in transverse sections, which is 4.06 μm ± 0.3. T - this is the section thickness, which is 1 μm. K - this is the diameter of the smallest recognisable fragment, which is assumed to be 0.5 μm. These parameters have to be inserted into the following formula to obtain the correction factor $f_{T.Goblet}$:

$$f_{T.Goblet} = \frac{a_0}{b_0} * \frac{[T+2*(r_N-K)]}{[T+2*(r_M-K)]} = \frac{3.9}{13.9} * \frac{[1+2*(3.5-0.5)]}{[1+2*(4.05-0.5)]} = 0.25\pm0.04.$$

time of 11-12 hours with a range of 10-14 and an S-phase duration of 8 hours. The G_2 plus M phase is assumed to be 2 hours for all cells. The G_1 phase is assumed to vary stochastically to generate the variation in the cell cycle duration. The labelling of S-phase cells with tritiated thymidine in the model is achieved by marking specific S-phase cells and this marker is transferred to all daughter cells derived by division. The dilution of label is not considered since, on the whole, short time scales are involved.

(4) Cell movement. It is assumed that cell movement, or migration, is the consequence of cell division. After division, one of the daughter cells remains in the same position as the mother cell while the other daughter is positioned immediately beneath its oldest immediate neighbour cell. This process we refer to as an age-dependent neighbour-selection process (see Loeffler et al., 1986). Following division all cells in the cell column in which the new cell is placed are shifted upwards one cell position, thus giving rise to the polarised overall cell movement up the crypt.

Assumptions for model extension

(5) Goblet cell lineage. The goblet cell lineage is assumed to originate from a proliferating transit columnar cell of a particular generation age (e.g. T3 or T4). The properties of goblet cells are assumed to be acquired with a certain probability at this stage (a stochastic switch). Once the transit cell has passed this point with-

out having switched into the goblet differentiation pathway, it will continue its development as a columnar epithelial cell. The cells that have acquired goblet properties are assumed to undergo no more than the same number of cell divisions as the corresponding columnar cell from which the lineage is derived. The mature, non-dividing goblet cells are called G cells. The cell kinetics of the proliferating goblet cells (g cells) are assumed to be the same as those of the other transit columnar cells (T cells). It is also assumed that the newly differentiated goblet cells behave in the same way as the columnar cells with respect to cell displacement following division (in an age-dependent neighbour-selection manner).

Fig. 3 shows, in a diagrammatic way, the crypt matrix including all the cell types and whether or not they are labelled (P, A, T1,...T6, M, g, G; * for labelling). Such a matrix can be analysed to give the positional frequency of g cells and G cells (PF_{Gob}) and a labelling index of g cells (LI_{Gob}). It can also be analysed to give information on the number of goblet cells appearing as singles or adjacent pairs or triplets in columns (Cl_{Gob}).

The model crypt matrix shown contains 364 cells while a true crypt contains about 235 cells (Potten et al.,1988). However, about 24 and 16 cell nuclei can be scored in longitudinal and transverse sections, respectively. Multiplication of these gives 384 from which some have to be subtracted due to the tapering at the bottom of the crypt. Evidently the model matrix should not be compared with whole crypt measurements but, rather, with a series of section measurements.

Technical details of the model simulations

The technical details of the model simulations have been presented extensively elsewhere (Loeffler et al., 1986, 1988; Potten and Loeffler, 1987). However, here we use some specific modifications. Recently, Chwalinski and Potten (1989) reported that within a crypt the spatial distribution of the Paneth cells is fairly homogeneous when one side is compared with the other. The position of the highest Paneth cell differed by no more than one cell position on either side of the crypt. This small intracryptal variation of Paneth cell positioning contrasts with a fairly high intercryptal variation where the position of the highest Paneth cell could be as low as position 2 in some cases or as high as position 7 in others. Based on these data, the positional frequency of Paneth cells had to be remodelled compared with our previous study (Loeffler et al., 1986, 1988). A data base of Paneth landscapes was created that was consistent with the properties just described for both individual crypts and different crypts. From these simulations a random sample of Paneth cell landscapes was drawn and on top of these landscapes, the appropriate number of stem cells were placed.

All subsequent simulations in this paper were performed with four actual stem cells unless otherwise specified. We have used a slightly modified version of the migration velocity of cells at the level of the crypt orifice namely, 0.7 cell positions per hour, instead of an earlier value of 1 cell position per hour. To adjust for this difference, the number of transit cell divisions (L) was fixed at 5.5 if four stem cells were used, or 4.5 if eight stem cells were used. The value of L used previously in these situations would have been 6 and 5, respectively.

The acquisition of goblet cell properties was assigned at random with a specified probability (P) to any newly generated transit columnar cell. This probability was assumed to be generation-age-dependent and for reasons of simplicity, this probability was set to 0 for all cell stages except one (i.e. only for population T3, $P3$=0.05). Technically, a separate cell division counter (generation-age counter) was introduced for the goblet cell lineage. After a goblet cell lineage is initiated, the generation-age counter takes the same value as the corresponding columnar sibling cell. This allows one to investigate differing lengths of the columnar and

gobl. cells [%]	LI total	LI goblet															cell position
6.25	0.00	0.00	M	M	M	M	M	M	M	M	M	M	M	G	M	M	M	M	24
12.50	0.06	0.00	M	G	M	M	M	M	M	M	M	M	M	G	M	6*	M	M	
6.25	0.00	0.00	M	G	M	M	M	M	M	M	M	M	M	M	M	M	M	M	
12.50	0.06	0.50	M	M	M	M	M	M	M	M	M	M	g*	G	M	M	M	M	
6.25	0.06	0.00	M	M	M	M	M	M	M	M	M	G	M	M	6*	M	M	M	20
12.50	0.06	0.50	M	M	M	M	M	6	M	M	5	5	G	g*	M	M	M	M	
6.25	0.19	1.00	M	M	M	M	M	6*	M	M	M	6*	M	g*	M	M	M	6	
6.25	0.25	0.00	M	M	M	M	M	G	M	6*	6*	M	M	6*	6*	M	M	M	
6.25	0.19	0.00	M	M	M	M	M	M	M	M	M	6	6*	6*	6*	M	M	G	
6.25	0.19	0.00	M	M	M	M	M	g	5	5*	5*	M	6*	M	M	M	6	M	15
6.25	0.06	0.00	M	M	M	M	G	M	M	M	M	5*	M	M	6	5	M	M	
0.00	0.50	----	5*	5*	5*	M	6*	M	6*	6*	M	M	M	M	6*	5	M	5*	
6.25	0.31	1.00	5*	5*	M	M	6	M	g*	M	M	M	M	6	6	6*	M	5*	
12.50	0.50	1.00	5*	5*	g*	M	4*	6*	M	g*	5*	M	6*	6	M	M	M	M	
12.50	0.25	0.50	M	5*	g	g*	6	6	M	M	5*	M	6	6	M	M	6	5*	10
6.25	0.31	0.00	g	5*	4*	4*	M	M	M	M	5	5*	5*	6	M	M	M	5	
6.25	0.63	0.00	g	4*	2*	2*	4*	6	6	4*	4*	5*	5*	5	6	4*	4*	4	
0.00	0.88	----	5*	5*	1	4*	M	3*	4*	4*	4*	3*	3*	3*	3*	3*	4*	4*	
0.00	0.38	----	M	P	A*	P	M	3	3*	4*	5	5	1	3*	3*	2*	5	5	
0.00	0.44	----	P	P	P	P	P	3	1*	4*	4*	P	A*	P	3*	1*	2*	4	5
0.00	0.06	----	P	P	P	P	P	P	A*	P	P	P	P	P	P	A	P	P	
0.00	0.00	----	P	P	P	P	P	P	P	P	P	P	P	P	P	P	P	P	
0.00	0.00	----				P	P	P	P	P	P	P	P	P	P				
0.00	0.00	----							P	P									
goblet singles:			0	0	0	1	1	2	1	1	0	1	2	1	0	0	0	1	
goblet pairs:			1	1	1	0	0	0	0	0	0	0	0	2	0	0	0	0	

Fig. 3. Diagram of the crypt represented as a 16 × 24 matrix (see Loeffler et al., 1986, 1988; Potten and Loeffler, 1987). P, Paneth cells; A, stem cells; transit generations 1-6; M, mature columnar cell; g, proliferating goblet cell; G, goblet cell; asterisk indicates cells labelled using tritiated thymidine. The percentage of goblet cells in each row is shown on the left, and the actual total labelling index and the goblet labelling index is also shown. At the base, the goblet clusters are shown.

goblet cell lineages by introducing terminal maturation (a transition to non-proliferating status, M or G, respectively) after different numbers of generations (L(G) ≤L(T)). The importance of these considerations will be discussed below.

The evaluation of the goblet labelling index (LI_{Gob}) is a simple extension of the overall LI evaluation, which is in this case restricted to g cells only. The evaluation of clusters of singles, adjacent pairs and triplets in the vertical column takes both g and G cells into account (see Fig. 3). The goblet clustering is referred to as Cl_{Gob}.

RESULTS

Experimental results

Fig. 4 summarizes a new set of experimental data from sections of the ileum of BDF1 mice specifically obtained for

this analysis. Fig. 4A shows the overall labelling index (LI) on a cell positional basis for the crypt obtained 40 minutes after injection of [^{3}H]TdR. Fig. 4B shows the frequency of goblet cells (PF_{Gob}) in these sections before any correction for centripetal position and size. The score of goblet cells when uncorrected reaches 25% in the middle regions of the crypt and shows a fall-off in the upper regions of the crypt. Fig. 4C shows the labelling index of the goblet cells in relation to cell position (LI_{Gob}). The labelling index for the goblet population shows a similar positional pattern to the overall labelling index (see Fig. 4A) with a significantly lower maximum value. It was not investigated whether this is due to differing cell kinetics of goblet and columnar cells. Due to difficulties in distinguishing between Paneth cells and goblet cells in the lower regions of the crypt with the PAS staining, we have ignored data for cell positions 1-7 in Fig. 4C. Fig. 4D gives data on the clustering pattern of goblet cells (Cl_{Gob}). About 80% of all goblet cells in the crypt sections appear as single individual cells, about 12% as adjacent pairs and a minority of less than 5% as triplets (i.e. three consecutive goblet cells in the vertical axis).

Due to the centripetal positioning of the mucus, goblet cells tend to be overscored in longitudinal sections of the crypt. Two ways of correcting this bias have been investigated leading to very similar results. The first measures the position and geometry of mucous bodies in a direct way as is illustrated in Fig. 2. The legend of this Figure provides the numerical data on the radial position and the size of the mucus-staining bodies. The estimated value of the factor f_T calculated with these parameters is 0.25 ± 0.04 (s.e.m.) indicating that the goblet cells are overscored by a factor of about 4.

An alternative, more empirical way of defining the correction factor is by comparing the cell counts (ratio of goblet cells to all cells) of the whole crypt with the cell counts of the sections. The absolute count of goblet cells in the whole crypt using PAS + AB staining is 12.92 ± 0.86, and the total cell number per crypt is 235 ± 9 (Potten et al., 1988), which gives a ratio of 0.055 ± 0.004. This Figure can be compared with the similar value derived from section material. The numbers are 5.0 ± 0.2 goblet cells per crypt section and 21.35 ± 0.54 for the average length of the crypt section. This gives a ratio of 0.235 ± 0.01. A comparison of 0.055 and 0.235 gives a value for the correction factor f_T of 0.23 ± 0.02. The similarity of this value with that derived from section diameter and positioning measurements above confirms the validity of these measurement approaches. Subsequently, positional goblet cell counts (PF_{Gob}) are corrected by a factor of 0.25 when comparisons are made with the model simulations. No corrections will be applied to the goblet labelling index and the goblet clustering data since these parameters represent ratios of goblet cell scores where correction factors cancel in first order approximation.

Taking these correction factors into account one can estimate that in the middle crypt region about 6% of all cells are goblet cells. At higher positions in the crypt close to the orifice the corrected data would indicate a number of 3%.

To investigate whether goblet cells really become less frequent with higher positions in the crypt, as indicated by

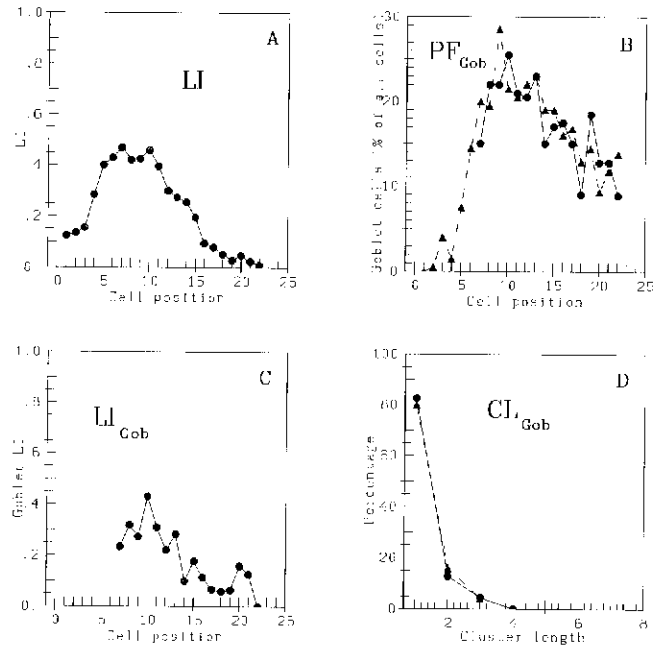

Fig. 4. Experimental data obtained from sections of the ileum of BDF1 mice. Data are obtained from two independent experiments (triangles, circles): (A) positional labelling index (LI) 40 minutes after injection of [^{3}H]TdR; (B) positional frequency of goblet cells (PF_{Gob}) (uncorrected for overscoring due to centripetal positioning of the mucus); (C) positional labelling index of goblet cells (LI_{Gob}) 40 minutes after injection of [^{3}H]TdR; (D) percentage of goblet cells appearing as singles, adjacent pairs, triplets (clusters) in crypt sections (CL_{Gob}).

the scores shown in Fig. 4B an additional scoring of goblet cells was undertaken on the villi. Fig. 5 shows goblet cells on a representative whole mount of a villus. Quantification shows that 9.92 ± 0.27 of all the cells on the villus are mucus-producing cells. This suggests that the decline in the positional score of mucus-producing cells with higher positions in the crypt should be interpreted with caution. We believe that the decline is attributable to indistinguishability of separate mucous globules and/or loss of globules due to physical friction at the narrow orifice of the crypt and/or temporary cessation of mucus production at the crypt-villus junction.

Results of model simulations

The model simulations were used to select concepts about the origin and development of the goblet cell lineage that are consistent with the data. Several model scenarios have been considered.

Reference scenario

First we describe a particularly simple model scenario, which already exhibits a good fit to some of the experimental data. It will be referred to as the 'reference scenario'.

Fig. 6A-D shows model simulations compared with the experimental data (corrected for overscoring where appropriate) using the following properties: (i) with a probability of 5%, any cell of the transit cell population T3 can dif-

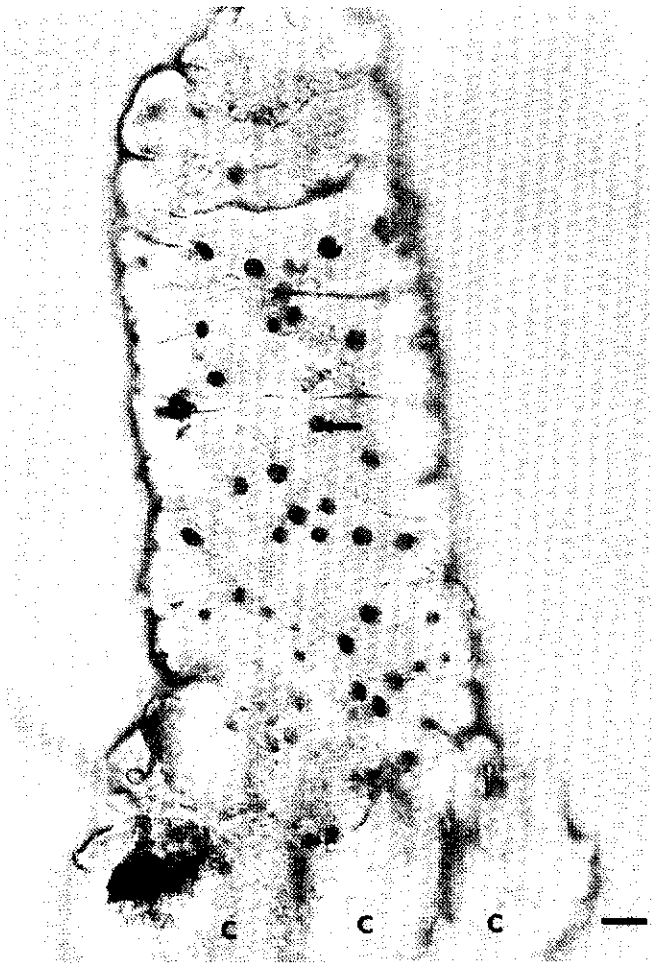

Fig. 5. Goblet cells on the villus epithelium stained with alcian blue (arrow). Many such areas were analysed by differential scoring of goblet cells and other epithelial cells. A number of crypts (C) can be seen attached to the base of the villus, although their goblet cells are toward the centre of the crypt, out of focus, and so are difficult to see in this Figure. Bar, 20 μm.

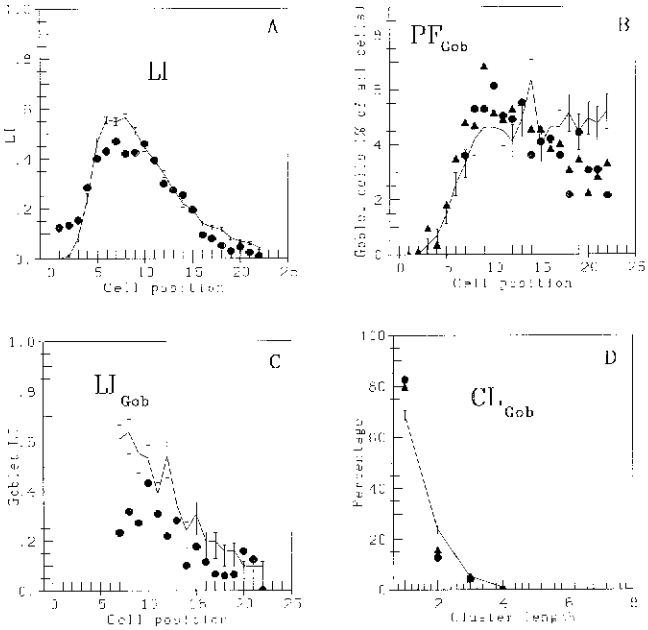

Fig. 6. Comparison of experimental data with model simulations assuming the reference scenario (see text and Fig. 7). Data are presented for two different experiments (triangles, circles, see Fig. 4). The model simulations (lines) were obtained on the basis of Monte Carlo simulations of 100 crypts. The aggregate scores are shown as means ± s.e.m. of the simulations. (A) positional labelling index (LI); (B) positional frequency of goblet cells (PF_{Gob}) data being corrected for overscoring due to centripetal positioning of the mucus (see text); (C) positional labelling index of goblet cells (LI_{Gob}); (D) percentage of goblet cells appearing as singles, adjacent pairs, or triplets (clusters) in crypt sections (CL_{Gob}).

ferentiate into a goblet cell; and (ii) once in the goblet lineage such cells undergo as many cell divisions with the same cell kinetic properties as all other columnar cells before becoming mature non-proliferating goblet cells (G cells). Thus, columnar and goblet cells do not differ in any kinetic aspect in this reference scenario. Simulations were run on 100 model crypts and the means and s.e.m. from the simulations are plotted in Fig. 6. The overall LI from Fig. 4A is shown in Fig. 6A, with a good fit between simulation and data. Fig. 6B shows the positional goblet cell counts corrected by the factor f_T=0.25. The maximum number of goblet cells reaches about 6% at cell position 10. At higher positions in the crypt, this percentage falls to about 3% at the top of the crypt. The model simulations show a good fit at low and middle crypt positions but no decline at higher positions. Fig. 6C shows the goblet labelling index from Fig. 4C and the model simulations. The simulations show higher values than the data in the mid-crypt region. Choosing slightly different cell kinetic parameters for the goblet cells (e.g. slightly longer cell cycle times) in the model would improve the fit. Fig. 6D compares the goblet clustering data from Fig. 4D with the model simulations. The model generates many more single goblet cells than pairs or even larger clusters. However, the percentage of goblet cells appearing as singles in the simulations is somewhat less than actually observed. This discrepancy can largely be attributed to the discrepancy already discussed in Fig. 6B. As the model scenario generates more cells (at the top positions of the crypt) than are actually scored, the chance of generating pairs in model columns is increased.

Fig. 7 schematically describes the cellular pedigree used in the above model simulations, assuming four stem cells per crypt. Differentiating cells undergo 5 or 6 transit cell divisions (5.5 on average) irrespective of whether they become columnar or goblet cells. It was assumed that the goblet cell property is acquired after passing the transit generation T3 with a probability of 5%. The transit goblet cells (g1, g2, g3) undergo as many additional transit cell divisions as their columnar counterparts (2.5 on average). The decision whether T5 or g2 transit cells undergo one extra cell division or not before maturing (becoming non-proliferative) was assumed to be stochastic with a probability of 50%. Therefore, it should be noted that the only new assumption introduced with respect to the goblet cell lineage is that the respective property is adopted at a specific

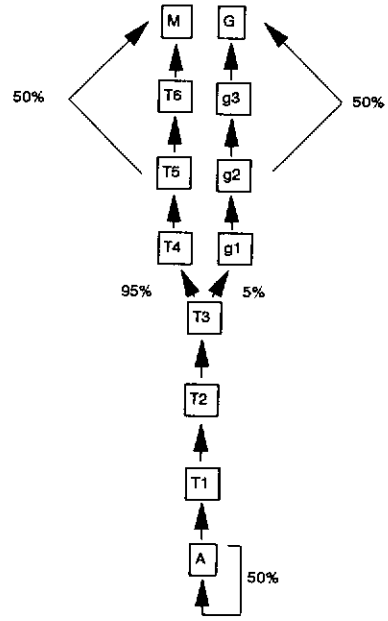

Fig. 7. Pedigree of the reference model scenario. The diagram schematically displays the cellular pedigree used in the model simulations shown in Fig. 6. Differentiating cells undergo 5 to 6 transit cell divisions irrespective of whether they become columnar or goblet cells. It was assumed that the goblet cell property is acquired after passing the transit generation T3 with a probability of 5%. The transit goblet cells (g1, g2, g3) undergo as many additional transit cell divisions as their columnar counterparts. The decision whether T5 or g2 transit cells undergo one extra cell division or not before maturing (becoming non-proliferative) was assumed to be stochastic with a probability of 50%.

step in the differentiation process and that other properties like cell kinetics are not affected.

Model variants

The reference model shown in Fig. 6B did not reproduce the decline in the goblet cell number at high crypt positions. As pointed out above this decline could be explained in various ways. An additional possibility for explaining this effect is based on the pedigree concept. Fig. 8A,B shows simulations obtained with a modified cellular pedigree. In contrast to the scheme displayed in Fig. 7 it was assumed that the number of transit divisions in the goblet cell pedigree is one cell division less than for the columnar transit cells, i.e. columnar cells amplify more at higher positions in the crypt than goblet cells. Fig. 8A shows that very satisfactory fits to the positional goblet cell frequency (PF_{Gob}) can be obtained. In addition, these simulations yield a perfect fit to the cluster data (Fig. 8B, full line). However, the LI generated by this model is unsatisfactory at high cell positions (not shown) and the model cannot explain the high level of goblet cells on the villus without additional assumptions. In fact, this model variant would not generate more than 3% goblet cells at the crypt orifice.

Fig. 8 also shows simulations of model variants that can be rejected as unacceptable. We here restrict our attention to variations of the pedigree only. Fig. 8B (broken line) shows the effect of increasing the number of generations in the goblet lineage to 4.5 (i.e. lowering the origin of the goblet lineage to the T1 columnar cell compartment, see Fig. 7). This results in considerable clustering of goblet cells, which is clearly not consistent with the data. More extensive simulations along this line show that scenarios with more than 3 generations in the goblet lineage are inconsistent with the high frequency of single goblet cells in the crypt.

On the other hand, very short goblet cell pedigrees are also unlikely. Fig. 8C shows the results for LI_{Gob} of a simulation with a goblet cell pedigree of only one transit generation originating at the T3-level (see Fig. 7), i.e. on average 1.5 divisions less than in the reference scenario. It is evident that such a scenario generates very few labelled goblet cells, i.e. the positional labelling index is far too low compared with the data.

Fig. 8D shows an example where the origin of the goblet cell pedigree was modified in the model. Instead of originating at the T3-level (see reference scenario) the origin was set at the T1-level (broken line) or at the T5-level (full line). Clearly, in the first case goblet cells would be predicted in lower crypt positions than were actually observed. In the second case, in contrast, one would hardly expect to find any goblet cells below cell position 8. More extensive simulations along these lines were undertaken and indicate that the goblet cell pedigree must originate 2 or 3 transit cell generations before the switch to the non-proliferative stage. When only four actual stem cells are present in a crypt this implies a differentiation at the T3-level (±1), when eight actual stem cells are present this would correspond to a differentiation at the T2-level (±1).

Table 1 summarises the results obtained using other simulations or model scenarios covering a broad range of options for the goblet cell pedigree. These scenarios were all designed to generate the same numbers of goblet cells in mid-crypt regions. To achieve this, the probabilities for generating goblet cells at the various positions were adjusted. Scenarios consistent with the experimental data are boxed. Comments are given as to why the other scenarios can be rejected based on the data observed. In particular it should be noted that if there are only four actual stem cells, then goblet lineages originating at the T2, T1, or even A-cell level generates curves that are not compatible with the data, i.e. the goblet cells are unlikely to have their own stem cells if we assume that the number of actual stem cells per crypt is less than 16 (or less than eight, on average).

DISCUSSION

The major conclusion that can be drawn from the present studies is that the pedigree concept of epithelial cell differentiation has been tested again and has withstood a further critical challenge. A specific pedigree for goblet cell differentiation could be derived. In agreement with the unitarian hypothesis (Cheng and Leblond, 1974), we also conclude that columnar and goblet cells originate from a common stem cell located at the crypt base. After 1-3 transit cell divisions (dependent on the number of stem cells), an irre-

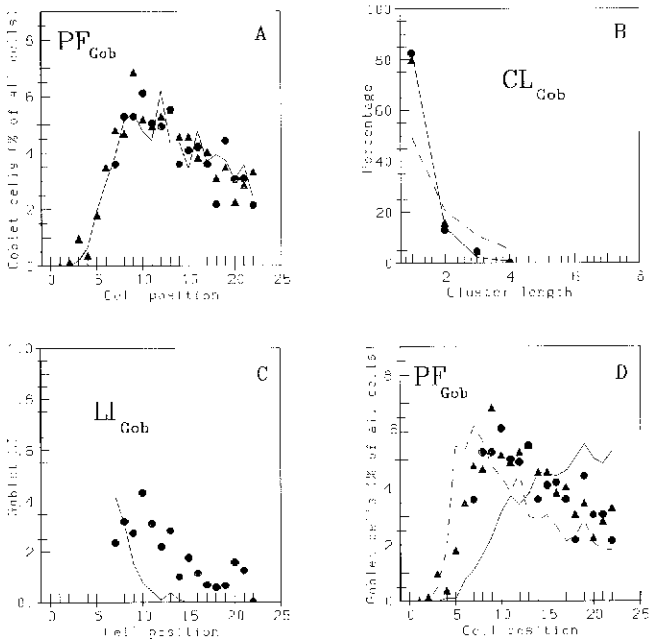

Fig. 8. Comparison of experimental data with model simulations assuming variations of the reference scenario (see text). Data and simulations are displayed as described in Fig. 6, except for error bars, which have been omitted for simplicity. The following model scenarios vary the origin and length of the goblet cell pedigree: (1) Origin of the goblet cells at T3 and goblet cell pedigree one cell division less than the columnar cells pedigree results in a decline in the positional goblet cell frequency at high positions and an ideal fit to the cluster data (Fig. 8A, Fig. 8B full line); (2) Origin at T1 and goblet and columnar cell pedigree with equivalent length results in large clusters (Fig. 8B, broken line); (3) Origin at T3 and only one transit goblet cell generation results in an unsatisfactory fit for the LI_{Gob} (Fig.8C, full line); (4) Origin at T1 and 3 transit goblet generations results in a PF_{Gob}, which rises at unrealistically low positions (Fig. 8D, broken line); (5) Origin at T5 and 0.5 transit goblet generations results in a PF_{Gob}, which rises at unrealistically high positions (Fig. 8D, full line).

versible differentiation event occurs, which distinguishes the columnar and goblet cell lineages. These two cell types continue their pedigree development with similar cell kinetics. The differentiation process can be described as stochastic. These conclusions suggest that the cellular development process is organised in a conditional fashion with the following rules being applied: (1) once a cell has reached stage T3, there is an option for it to proceed as a columnar cell or a goblet cell. (2) Once past this decision point, the decision is irreversible. (3) The decision made at this point then determines the further pedigree development. It is easy to envisage genetic processes generating such diversity. From our point of view, an appealing feature of these results is the fact that they can be easily explained within the framework of our previously developed model with an age structured epithelial cell development.

The decline in the number of goblet cells towards the top of the crypt was an unexpected experimental finding. However, a literature search revealed a similar finding in rats by Becciolini et al. (1985). The modelling could provide an explanation for this fall in the proportion of goblet cells if approximately one of the transit cell divisions in the

Table 1. Summary of modelled scenarios

N(A)	4 stem cells/crypt					
Tc(A)	16 hours					
Tc(T,G)	11 hours/12 hours					
L(T)	5.5					
L(G)	0	0.5-1	1.5-2	2.5-3	3.5-4	4.5
Origin(G)	T1 32% T2 22% T3 15% T4 10% T5 7% T6 7%	T1 15% T2 11% T3 8% T4 6% T5 5%	T1 8% T2 7% **T3 6%** **T4 5%**	T1 6% T2 6% **>T3 5%<**	T1 5% T2 5%	T1 5%
Comment	No labelled goblet cells	Goblet LI too short	T1,T2: inconsistent with cell position data		Goblet singles too rare	Goblet singles too rare

N(A), number of stem cells; Tc(A), cell cycle time of stem cells; Tc(T,G), cell cycle time of columnar and goblet cells; L(T), average number of columnar cell generations; L(G), average number of goblet cell generations.
>T3 5%<, reference case; acceptable cases in bold.

goblet lineage were omitted compared with the columnar cell lineage. On the other hand this is contradicted by the high number of mucus-producing cells on the villus. Thus, other explanations for the observed changes in the frequency of goblet cells with increasing position are more likely: (1) transient and variable levels of mucus secretion during the course of goblet maturation and migration, i.e. the switching on and switching off of mucus production as has been discussed by Neutra and Leblond (1966) on the base of rat data. (2) Physical friction near the orifice of the crypt removing some of the mucous globules. (3) Difficulty in distinguishing between adjacent mucous globules in the narrow region near the crypt orifice thereby leading to underscoring.

We recognise that the model suffers from a number of simplifications and these have been discussed in detail elsewhere (Loeffler et al., 1986, 1988; Potten and Loeffler, 1987). In brief, the simplifications are as follows: (1) the crypts all have the same size and number of stem cells - this is clearly an over simplification. (2) A square lattice is used, which ignores changes in shape of the crypt cylinder at the top and also ignores the more likely hexagonal packing of cells. (3) Cell movement in the absence of mitosis is not possible in the model, but clearly can occur in a real crypt. (4) Cell movement results in an entire column of cells being displaced vertically, i.e. all the cell contacts with the neighbouring cell columns have to be broken and remade. (5) The goblet cell lineage originates from one specified T-cell generation only. A further limitation of the model is the fact that it cannot describe the recovery of the crypt after serious damage. As a consequence of this, alternative modelling techniques have to be applied (Paulus et al., 1992). In addition, the present model does not provide for crypt fission, crypt extinction, nor for the crypt life-cycles over long time scales. Here, again, other types of models have to be adopted (Loeffler and Grossman, 1991), which can provide fits to the known estimates of crypt fission, suggested extinction frequencies and provide size distribution data for the entire crypt if the average number of stem cells is assumed to be at least four. Recent data of Hendry

et al. (1989) provided independent evidence that the number of actual stem cells could indeed be as low as four. Simulations performed with the model, including goblet cell differentiation, showed that basically similar sets of model curves and, hence, conclusions could be generated assuming eight stem cells per crypt.

In the present model, the decision of a transit cell to differentiate down the goblet lineage was assumed to be stochastic. This yields a wide spatial spread of the goblet cells throughout the crypt. However, there is no biological evidence for, or against, this assumption about a stochastic decision and it may be worthwhile to investigate this and possible mechanisms further. The model would suggest that if the probability of a particular sensitive transit cell stage (e.g. T3) to differentiate to a goblet cell is 0.05, then the probability of finding crypts that contain no goblet cells at all could also be calculated. This would be achieved if 3 or 4 successive T3 generations in one crypt do not produce a single goblet cell. Under these circumstances, at least 2% of all crypts should be goblet cell-negative and this should be a detectable quantity. It would be interesting to exclude this possibility as it would indicate that there is some regulatory process guaranteeing a minimum number of goblet cells in each crypt. The pedigree concept would also predict that crypts regenerated following serious stem cell injury such as irradiation would exhibit a similar time scale for the recovery of the columnar cells and the goblet cell populations.

We have presented here some new experimental data. We have determined the magnitude of the overscoring (fourfold) of goblet cells in sections. We have used two independent methods and these give comparable results. The absolute value of this correction factor has an impact on the numerical value that we use in the model for the goblet cell differentiation probability. Thus, any error in the correction factor affects the numerical values for this probability. We have been unable to detect any clear evidence that this number changes with increasing cell position in the crypt. However, this particular question has not been addressed in detail.

The experimental data for the goblet LI and the goblet clustering have not been subjected to any correction. For the goblet-labelling index, the argument is that the labelled and unlabelled goblet cells should have similar sizes and positioning effects and, therefore, this will not considerably effect the ratio. Similarly, the numbers for the clustering patterns are not corrected as they represent relative proportions amongst similar cells.

The number of goblet cells has been reported to differ depending on the region of the murine gut being investigated (Cheng and Leblond, 1974; Merzel and Leblond, 1969; Cheng, 1974). We have studied, in our experiments, an average crypt in the mid-ileal region. For the modelling, one might have to adjust for any different shapes and geometries of the crypt and the different cell-cycle parameters, different numbers of stem cells and differing lengths of pedigrees in other regions. The number of goblet cells clearly differs considerably in the large bowel compared to the small bowel. We are in the process of analysing similar data (to those presented here) generated for the colonic epithelium.

The reference model simulations for the labelling index of goblet cells (LI_{Gob}) displayed in Fig. 6C is higher than actually found in the data. This discrepancy suggests that the proliferating goblet cells have a slightly different cell cycle characteristic to the columnar cells from which the model parameters where obtained (e.g. shorter S-phase or longer cell cycle time).

Bjerknes and Cheng (1985) performed [^{3}H]TdR labelling studies to investigate the clustering of newly produced goblet cells. They found that pairs of labelled goblet cells originate in the crypt several hours after injection of [^{3}H]TdR. This supports our concept of symmetric cell divisions in the goblet pedigree. The migration process then separates these goblet cell pairs and generates single goblet cells. In fact, they found that goblet cells appear as single cells on the villus. Thus, our model gives a natural explanation of their findings.

There is an indication of species dependency of the goblet cell pedigree. Cairnie (1970) was unable to detect proliferating goblet cells in the small intestine of rats. However, he reported that labelled goblet cells could be generated when he applied [^{3}H]TdR several hours before sampling. Based on our model reasoning we hypothesize that the goblet pedigree in rats originates at the last columnar cell division directly generating non-dividing mucus-producing cells. Such a pedigree would be similar to the one simulated in Fig. 8D (full line, see above). This was rejected regarding our own data for mice, which showed a rise at low positions. However, the positional goblet cell numbers scored by Cairnie show that the goblet cells appear at much higher positions in the crypt, thereby supporting our hypothesis.

This work has been supported by Deutsche Forschungsgemeinschaft (Grant LO342/4-1 to M.L.) and the Cancer Research Campaign (U.K.). We are particularly grateful to the British Council and the German DAAD for their support over several years.

REFERENCES

Becciolini, A., Fabrica, D., Cremonini, D. and Balzi, M. (1985). Quantitative changes in the goblet cells of the rat small intestine after irradiation. *Acta Radiol. Oncol.* **24**, 291-299.

Bizzozero, G. (1892). Über die schlauchförmigen Drüsen des Magendarmkanals und Beziehungen ihres Epithels zu dem Oberflächenepithel der Schleimhaut. *Arch. Mikrosc. Anat.* **40**, 325-375.

Bjerknes, M. and Cheng, H. (1985). Mucous cells and cell migration in the mouse duodenal epithelium. *Anat. Rec.* **212**, 69-73.

Cairnie, A. B. (1970). Renewal of goblet and Paneth cells in the small intestine. *Cell Tiss. Kinet.* **3**, 35-45.

Chang, W. W. L. and Leblond, C. P. (1971). Renewal of the epithelium in the descending colon of the mouse. *Amer. J. Anat.* **131**, 73-100.

Chang, W. W. L. and Nadler, N. J. (1975). Renewal of the epithelium in the descending colon of the mouse. IV. Cell population kinetics of vacuolated-columnar and mucous cells. *Amer. J. Anat.* **144**, 39-56.

Cheng, H. and Leblond, C. P. (1974). Origin, differentiation and renewal of the four main epithelial cell types in the mouse small intestine. V. Unitarian Theory of the origin of the four epithelial cell types. *Amer. J. Anat.* **141**, 537-61.

Cheng, H. (1974). Origin, differentiation and renewal of the four main epithelial cell types in the mouse small intestine. II. Mucous cells. *Amer. J. Anat.* **141**, 481-501.

Chwalinski, S. and Potten, C. S. (1989). Crypt base columnar cells in ileum of BDF1 male mice their numbers and some features of their proliferation. *Amer. J. Anat.* **186**, 397-406.

Cooper, J. W. (1974). Relative and absolute goblet cell numbers in intestinal crypts following irradiation or actinomycin D. *Experientia* **30**, 549-50.

Dellanna, F., Paulus, U. and Potten, C. S. (1989). The spread of clonally marked cells on intestinal epithelium provides insight into cell migration and stem cell organization by using model simulation. *Cell Tiss. Kinet.* **22**, 168 (abstract).

Gordon, J. I., Schmidt, G. H. and Roth, K. A. (1992). Studies of intestinal stem cells using normal, chimeric, and transgenic mice. *FASEB J.* **6**, 3039-3050.

Hendry, J. H., Potten, C. S., Ghafoor, A., Moore, J. V., Roberts, S. A. and Williams, P. C. (1989). The response of murine intestinal crypts to short-range promethium-147 beta irradiation: deductions concerning clonogenic cell numbers and positions. *Radiat. Res.* **118**, 364-74.

Inoue, M., Imada, M., Fukushima, Y., Matsuura, N., Shiozaki, H., Mori, T., Kitamura, Y. and Fujita, H. (1988). Macroscopic intestinal colonies of mice as a tool for studying differentiation of multipotential intestinal stem cells. *Amer. J. Pathol.* **132**, 49-58.

Kaur, P. and Potten, C. S. (1986). Circadian variation in migration velocity in small intestinal epithelium. *Cell Tiss. Kinet.* **19**, 591-599.

Leblond, C. P. and Messier, B. (1958). Renewal of chief cells and goblet cells in the small intestine as shown by radioautography after injection of thymidine-H3 into mice. *Anat. Rec.* **132**, 247-259.

Li, Y. Q., Fan, C. Y., O'Connor, P. J., Winton, D. J. and Potten, C. S. (1992). Target cells for the cytotoxic effects of carcinogens in the murine small bowel. *Carcinogenesis* **13**, 361-8.

Loeffler, M. and Grossmann, B. (1991). A stochastic branching model with formation of subunits applied to the growth of intestinal crypts. *J. Theor. Biol.* **150**, 175-91.

Loeffler, M., Potten, C. S., Paulus, U., Glatzer, J. and Chwalinski, S. (1988). Intestinal crypt proliferation. II. Computer modelling of mitotic index data provides further evidence for lateral and vertical cell migration in the absence of mitotic activity. *Cell Tiss. Kinet.* **21**, 247-58.

Loeffler, M., Stein, R., Wichmann, H. E., Potten, C. S., Kaur, P. and Chwalinski, S. (1986). Intestinal cell proliferation. I. A comprehensive model of steady-state proliferation in the crypt. *Cell Tiss. Kinet.* **19**, 627-45.

Merzel, J. and Almeida, M. L. (1973). Maturation of goblet cells of the mouse small intestine as shown by the uptake of ^{35}S-sodium sulfate. *Anat. Rec.* **177**, 519-24.

Merzel, J. and Leblond, C. P. (1969). Origin and renewal of goblet cells in the epithelium of the mouse small intestine. *Amer. J. Anat.* **124**, 281-305.

Neutra, M. and Leblond, C. P. (1966). Synthesis of the carbohydrate of mucus in the Golgi complex as shown by electron microscope radioautography of goblet cells from rats injected with glucose-H^3. *J. Cell Biol.* **30**, 119-136.

Paulus, U., Potten, C. S and Loeffler, M. (1992). A model of the control of cellular regeneration in the intestinal crypt after perturbation based solely on local stem cell regulation. *Cell Prolif.* **25**, 559-578.

Potten, C. S. (1990). A comprehensive study of the radiobiological response of the murine (BDF1) small intestine. *Int. J. Radiat. Biol.* **58**, 925-973.

Potten, C. S., Chwalinski, S., Swindell, R. and Palmer, M. (1982). The spatial organization of the hierarchical proliferative cells of the crypts of the small intestine into clusters of 'synchronized' cells. *Cell Tiss. Kinet.* **15**, 351-70.

Potten, C. S. and Hendry, J. H. (1985). The microcolony assay in mouse small intestine. In *Cell Clones: Manual of Mammalian Cell Techniques* (ed. C. S. Potten and J. H. Hendry), pp. 50-60. Churchill Livingstone, Edinburgh.

Potten, C. S., Kellett, M., Roberts, S. A., Rew, D. A. and Wilson, G. D. (1992). Measurement of in vivo proliferation in human colorectal mucosa using bromodeoxyuridine. *Gut* **33**, 71-78.

Potten, C. S. and Loeffler, M. (1987). A comprehensive model of the crypts of the small intestine of the mouse provides insight into the mechanisms of cell migration and the proliferation hierarchy. *J. Theor. Biol.* **127**, 381-91.

Potten, C. S., Roberts, S. A., Chwalinski, S., Loeffler, M. and Paulus, U. (1988). Scoring mitotic activity in longitudinal sections of crypts of the small intestine. *Cell Tiss. Kinet.* **21**, 231-46.

Sacerdotti, C. (1894). Über die Entwicklung der Schleimzellen des Magendarmkanals. *Int. Mschr. Anat. Physiol.* **11**, 501-514.

Tannock, I. F. (1967). A comparison of the relative efficiencies of various metaphase arrest agents. *Exp. Cell Res.* **47**, 345-356.

Winton, D. J., Blount, M. A. and Ponder, B. A. J. (1988). A clonal marker induced by mutation in mouse intestinal epithelium. *Nature* **333**, 463-66

(Received 14 April 1993 - Accepted 25 June 1993)